第 37 卷 第 3 期 原 子 核 物 理 评 论 Vol. 37, No. 3
2023 年 6 月 Nuclear Physics Review Jun. , 2023

Article ID: 1007-4627(2023) 03-0001-07

Systematics of 2_1^+ states in $N = 82$ even-even isotones

Q. Y. Chen[1], Y. X. Yu[1], S. T. Guo[1], G. J. Fu[1], Z. Z. Ren[1]

(*1. School of Physics Science and Engineering, Tongji University, Shanghai 200092, China*)

Abstract: In this paper, we study the systematics of the 2_1^+ states in the $N = 82$ even-even isotones with proton numbers between 52 and 72. We calculate the level energies of the 0_1^+, 2_1^+ states and the electric quadrupole reduced transition probabilities $B(E2; 2_1^+ \to 0_1^+)$, in the framework of the nuclear shell model with a monopole- and multipole-optimized realistic interaction. Our calculations yield good agreement with the experimental data and show a 2.5 MeV gap at $Z = 64$ subshell closure in ^{146}Gd. We predict that the $B(E2; 2_1^+ \to 0_1^+)$ value for ^{146}Gd is close to those for ^{142}Nd and ^{144}Sm, and the values increase rapidly from ^{148}Dy to ^{152}Yb.

Key words: shell model; $N = 82$ isotones; 2_1^+ state energy; electric quadrupole reduced transition probability

CLC number: O571.6 **Document code:** A **DOI:** 10.11804/NuclPhysRev.37.01.01

1 Introduction

The $N = 82$ isotones are one of the longest chains of neutron semimagic nuclei in nuclide chart. The systematics of the 2_1^+ states in the $N = 82$ even-even isotones with $Z > 50$ has attracted much interest. Previous experiments measured excitation energies of the 2_1^+ states [denoted by $E_x(2_1^+)$ in this paper] for ^{134}Te-^{154}Hf, and showed $E_x(2_1^+)$ in ^{146}Gd is much larger than those in any other $N = 82$ isotones [1], indicating the proton $Z = 64$ subshell closure for nuclei in this region [2]. As a comparison, in the proton semimagic Sn isotopes with $50 < N < 82$, the largest $E_x(2_1^+)$ is at ^{102}Sn, and $E_x(2_1^+)$ in ^{114}Sn is the second largest.

Another important observable for nuclear properties of low-lying states is the electric quadrupole reduced transition probabilities $B(E2; 2_1^+ \to 0_1^+)$. For example, in the Sn isotopes, there is a particular measurement of interest: the $B(E2; 2_1^+ \to 0_1^+)$ values, which show a shallow minimum at ^{116}Sn. This minimum has sparked significant attention among researchers [3-11] and was explained in two different ways: a result of a possible soft neutron $N = 64$ subshell closure [10], or due to proton excitation from the $0g_{9/2}$ orbit [11]. For the $N = 82$ isotones, the measured $B(E2; 2_1^+ \to 0_1^+)$ values first increase from ^{134}Te to ^{140}Ce and then stay nearly constant up to ^{144}Sm. Unfortunately, no measurements exist for isotones with $A > 144$. This raises the question of whether a shallow minimum in $B(E2; 2_1^+ \to 0_1^+)$ exists at $Z = 64$ for the $N = 82$ isotones.

In order to comprehensively understand the evolution of proton shell structure in $N = 82$ isotones, theoretical efforts have been devoted to the systematical study of the 2_1^+ states. For example, Holt *et al*. [12] performed shell model and QRPA calculations. Their results showed that, using a realistic interaction derived from the meson-exchange potential, the shell model predicted a slight increase in the $E_x(2_1^+)$ values from ^{134}Te to ^{146}Gd. On the other hand, the QRPA calculation produced a constant $E_x(2_1^+)$ value. Coraggio *et al*. [13] performed shell model calculations using a realistic interaction derived from the CD-Bonn potential. They showed a maximum $E_x(2_1^+)$ value at ^{148}Dy.

The purpose of this paper is to study the systematics of the 2_1^+ states for the $N = 82$ even-even isotones, in the framework of the shell model. We calculate the $E_x(2_1^+)$ values and $B(E2; 2_1^+ \to 0_1^+)$ transition strengths using a monopole- and multipole-optimized effective interaction that was recently developed in our previous work [14]. This paper is organized as follows. In Sec. 2 we give a brief introduction to the framework of shell model, the Hartree-Fock, and the particle number conserved BCS. In Sec. 3 we present our calculation results including the $E_x(2_1^+)$ values, relative binding

Received date: 19 Jun. 2023; **Revised date:** 19 Jun. 2023

Foundation item: the National Key R&D Program of China (2018YFA0404403); Natural Science Foundation of China (12075169,12035011, 11605122)

Biography: Q. Y. Chen and Y. X. Yu contributed equally to this work. Q. Y. Chen(1998-) and Y. X. Yu(1994-), Shanghai, Studying at Tongji University

Corresponding author: E-mail: gjfu@tongji.edu.cn

energies, and $B(E2;2_1^+ \to 0_1^+)$ transition strengths. We show our results are in good agreement with the experimental data. In Sec. 4 we summarize our results.

2 Framework

We perform full shell model (SM) calculations for ^{134}Te, ^{136}Xe, ^{138}Ba, ^{140}Ce, ^{142}Nd, ^{144}Sm, ^{146}Gd, ^{148}Dy, ^{150}Er, ^{152}Yb, and ^{154}Hf with valence protons outside doubly magic core ^{132}Sn in the $0g_{7/2}1d_{5/2}1d_{3/2}2s_{1/2}0h_{11/2}$ shell using the BIGSTICK code [15-16]. The maximum dimension of the SM calculation reaches 1.6×10^7 at ^{148}Dy. In our previous work [14], we derived a monopole- and multipole-optimized effective interaction based on the realistic JJ56PNA interaction [17].The Coulomb interaction between the protons is included in this interaction, similar to previous studies in Refs. [12] and [13]. This effective interaction reproduces the binding energies, low-lying level energies, the electric quadrupole moments, the electric quadrupole reduced transition probabilities, the magnetic dipole moments, and the magnetic dipole reduced transition probabilities for both the even-even and odd-mass nuclei with $N = 82$. In this work, we use this interaction to calculate 0_1^+- and 2_1^+-state level energies and the $B(E2;2_1^+ \to 0_1^+)$ transition strength. The electric quadrupole transition operator is defined by $\hat{T}(E2) = e_\pi \hat{r}^2 \hat{Y}_2$, where e_π is the effective charge of valence protons. We take $e_\pi = 1.6$ and the empirical formula of the harmonic oscillator length $b = (1.012A^{1/3})^{1/2}$ fm.

For comparison, we also calculate the ground state energies in the Hartree-Fock (HF) and the number conserved BCS (NBCS) [18-20] using the same effective interaction. We start with the HF calculation in the $0g_{7/2}1d_{5/2}1d_{3/2}2s_{1/2}0h_{11/2}$ shell with Kramers degeneracy, i.e., our HF calculation produces time reversal single-particle partners without enforcing additional constrains such as shape and orientation. The HF single-particle state obtained from the calculation can be written as a transformation of the SM single-particle states:

$$\hat{a}_\alpha^\dagger = \sum_a U_{\alpha a}\hat{c}^\dagger_{j_a m_a}. \tag{1}$$

Here U is the transformation matrix.

The building blocks of the NBCS are collective pairs in the HF basis, i.e.,

$$\hat{P}^\dagger = \frac{1}{2}\sum_\alpha v_\alpha \hat{a}_\alpha^\dagger \hat{a}_{\tilde{\alpha}}^\dagger, \tag{2}$$

where v_α is the pair structure coefficient. In the NBCS, the ground state of $2N$ valence protons is an N-pair condensate, i.e.,

$$|\phi\rangle = \frac{1}{\sqrt{\chi_N}}(\hat{P}^\dagger)^N|0\rangle, \tag{3}$$

where χ_N is the normalization factor. It is worth emphasizing that the particle number is exactly conserved in the NBCS state described in Eq. (3), which has similarities to the seniority-zero state in the generalized seniority scheme [21-23]. Unlike traditional BCS calculations in nuclear structure theory, the NBCS state does not require a numerical particle number projection.

The Hamiltonian of NBCS for valence protons can be written as

$$\hat{H} = \sum_{\alpha\beta}\varepsilon_{\alpha\beta}\hat{a}_\alpha^\dagger\hat{a}_\beta + \frac{1}{4}\sum_{\alpha\beta\gamma\delta}V_{\alpha\beta\gamma\delta}\hat{a}_\alpha^\dagger\hat{a}_\beta^\dagger\hat{a}_\delta\hat{a}_\gamma, \tag{4}$$

where $\varepsilon_{\alpha\beta}$ and $V_{\alpha\beta\gamma\delta}$ are single-particle energies and two-body matrix elements, respectively, in the HF single-particle basis. The energy of the NBCS state described in Eq. (3) can be written by

$$\begin{aligned} E &\equiv \langle\phi|\hat{H}|\phi\rangle \\ &= \sum_\alpha (2\varepsilon_{\alpha\alpha}+V_{\alpha\tilde{\alpha}\alpha\tilde{\alpha}})\left(1-\frac{\chi_N^{[\alpha]}}{\chi_N}\right) \\ &\quad + \sum_{\alpha\beta}^{\alpha\neq\beta}\left[V_{\alpha\tilde{\alpha}\beta\tilde{\beta}}N^2 v_\alpha v_\beta \frac{\chi_{N-1}^{[\alpha\beta]}}{\chi_N}\right. \\ &\quad \left. +(V_{\alpha\beta\alpha\beta}+V_{\alpha\tilde{\beta}\alpha\tilde{\beta}})\left(1-\frac{\chi_N^{[\alpha]}+\chi_N^{[\beta]}-\chi_N^{[\alpha\beta]}}{\chi_N}\right)\right]. \end{aligned} \tag{5}$$

Here $\sum_\alpha$ represents the summation over α or $\tilde{\alpha}$, where α and $\tilde{\alpha}$ are degenerate time-reversed pairs. $\chi_N^{[\alpha]}$ and $\chi_N^{[\alpha\beta]}$ are α- and $\alpha\beta$-orbit blocked normalization factors, respectively. The pair structure coefficient v_α is determined by minimizing the energy of the NBCS state. The formulae for the variational principle of the NBCS can be found in Refs. [18-19] and were extended to the case of open-shell nuclei in Ref. [20]. Since the $N = 82$ even-even isotones are nearly spherical nuclei, the result of the NBCS is very close to that of the generalized seniority scheme with seniority zero.

3 Results

Table 1 compares for the relative nuclear binding energies (the binding energy difference between the $N = 82$ nuclei and ^{132}Sn) from the experimental data, our full SM, HF, and NBCS. The relative binding energy data are derived by

Table 1　Nuclear binding energy difference (in MeV) between the $N = 82$ nuclei and ^{132}Sn. The theoretical values are obtained by our calculations of full SM, HF, and NBCS with the effective interaction in Ref. [14].

Nuclide	Expt.	SM	HF	NBCS
^{134}Te	20.548	20.552	19.319	20.548
^{136}Xe	39.004	39.019	36.985	38.993
^{138}Ba	55.396	55.421	53.016	55.363
^{140}Ce	69.767	69.792	67.410	69.697
^{142}Nd	82.200	82.228	78.748	82.079
^{144}Sm	92.771	92.846	89.434	92.617
^{146}Gd	101.446	101.568	99.300	101.275
^{148}Dy	107.774	107.936	104.482	107.645
^{150}Er	112.298	112.403	108.553	112.116
^{152}Yb	115.289	115.116	111.305	114.878
^{154}Hf	116.287	116.158	112.995	115.972

subtracting the electron binding energy from the atomic binding energy value compiled in the AME2020 database [24]. The relative binding energies obtained by our SM calculation are very close to the data, with a root-mean-square deviation of 98 keV. The relative binding energies obtained by the NBCS are in good agreement with the data and the SM result, but those obtained by HF are 1-4 MeV smaller. This indicates the pair correlation is very important here.

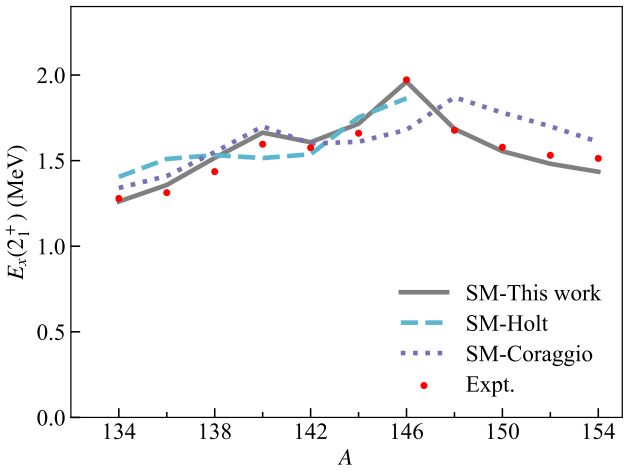

Fig. 1　The excitation energies of the 2_1^+ states, $E_x(2_1^+)$, for the $N = 82$ even-even isotones with $Z > 50$. 'SM-Holt" and "SM-Coraggio" represent the shell-model results in Refs. [12] and [13], respectively. The experimental data are taken from the ENSDF database [25].

Fig. 1 compares for the $E_x(2_1^+)$ values from the experimental data, the SM results in this work and in Refs. [12-13]. The data are taken from the ENSDF database [25]. We see for the entire range of the $N = 82$ even-even isotones, the $E_x(2_1^+)$ values obtained by our SM calculation are

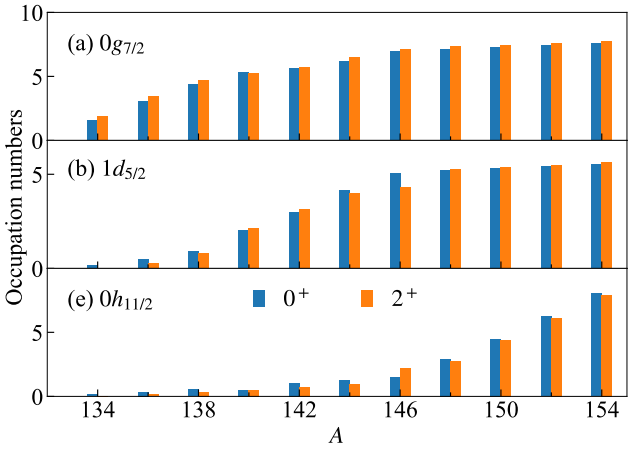

Fig. 2　The expectation value of the occupation number of the $0g_{7/2}$, $1d_{5/2}$, and $0h_{11/2}$ orbits in the 0_1^+ and 2_1^+ states.

in good agreement with the data, with a root-mean-square deviation of only 49 keV. The experimental data exhibit two distinct peaks of $E_x(2_1^+)$, with the highest peak observed at ^{146}Gd with an energy of 1.972 MeV, and the second peak at ^{140}Ce with 1.596 MeV. Our SM calculation successfully reproduces this phenomenon, with our values for the two peaks being 1.961 MeV and 1.664 MeV, respectively. On the other hand, the SM calculation in Ref. [13] predicted $E_x(2_1^+)$ in good agreement with the data for ^{134}Te-^{144}Sm, but it failed to reproduce the maximum peak at ^{146}Gd: the theoretical $E_x(2_1^+)$ value for ^{146}Gd is 0.3 MeV smaller than the data, and those for ^{148}Dy, ^{150}Er, and ^{152}Yb are $\sim$ 0.2 MeV larger than the data. The effective interaction used in Ref. [13] does not well reproduce the evolution of the proton shell structure. The calculation in Ref. [12] predicted $E_x(2_1^+)$ values increase slightly from ^{134}Te to ^{146}Gd, but the results for $A > 146$ were not reported.

The expectation value of the occupation number of the $0g_{7/2}$, $1d_{5/2}$, $1d_{3/2}$, $2s_{1/2}$, and $0h_{11/2}$ orbits is obtained by our SM calculation. The occupation numbers of the $1d_{3/2}$ and $2s_{1/2}$ orbits are very small in the 0_1^+ and 2_1^+ states of ^{134}Te-^{154}Hf. In Fig. 2 we see that the occupation numbers of the $0g_{7/2}$ and $1d_{5/2}$ orbits increase rapidly and approach the saturation values as A increases, while the number of the $0h_{11/2}$ orbit almost vanishes for $A < 146$ and subsequently increases. The occupation number of the $1d_{5/2}$ orbit in the 2_1^+ state of ^{146}Gd is 0.7 smaller than that in the ground state, whereas the occupation number of the $0h_{11/2}$ orbit in the 2_1^+ state is 0.7 larger than that in the ground state. The 2_1^+ state in ^{146}Gd is conventionally considered a one-phonon excitation of the 0_1^+ ground state or the generalized seniority two

[12]. The motion of the valence proton from the $1d_{5/2}$ to the $0h_{11/2}$ orbit plays a role in the formation of the 2_1^+ state.

In order to study the proton shell structure for the $N = 82$ isotones, we derive the HF single-particle energy for the SM orbit. The procedure is as follows. Using Eq. (1) we have

$$\varepsilon_{j_a m_a} = \sum_{\alpha} \left(U_{\alpha a}\right)^2 \varepsilon_{\alpha}, \tag{6}$$

where ε_α is the calculated single-particle energy of the HF orbit, and $\varepsilon_{j_a m_a}$ is the single-particle energy of the SM orbit. Our calculation shows that for the nearly spherical even-even nucleus with $N = 82$, the $\varepsilon_{j_a m_a}$ values with the same j_a but different m_a are close to each other. Based on this observation, we calculate the average $\varepsilon_{j_a m_a}$ value for each j_a but differing m_a:

$$\overline{\varepsilon}_{j_a} = \frac{1}{2j_a + 1} \sum_{m_a} \varepsilon_{j_a m_a}. \tag{7}$$

We assume that $\overline{\varepsilon}_{ja}$ represents the HF single-particle energy of the j_a orbit.

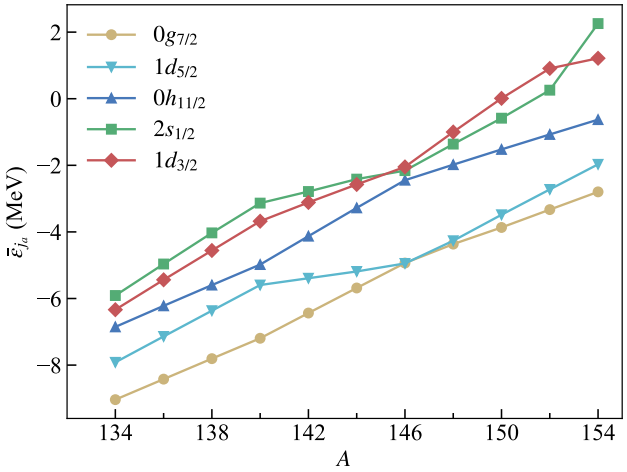

Fig. 3 The evaluated HF single-particle energy $\overline{\varepsilon}_{j_a}$ of the $0g_{7/2}$, $1d_{5/2}$, $1d_{3/2}$, $2s_{1/2}$, and $0h_{11/2}$ orbits.

Fig. 3 shows the results of the HF single-particle energies of the $0g_{7/2}$, $1d_{5/2}$, $1d_{3/2}$, $2s_{1/2}$, and $0h_{11/2}$ orbits in the $N = 82$ even-even isotones. We see a pronounced increase in the energies across the isotones ^{134}Te-^{154}Hf, with values ranging from −9 to −6 MeV at lower energies and increasing to −3 to 2 MeV at higher energies. This increase arises due to the repulsive monopole interaction between identical valence nucleons. We find a large gap between the $1d_{5/2}$ and $0h_{11/2}$ orbits in ^{146}Gd: the difference between $\overline{\varepsilon}_{1d_{5/2}}$ and $\overline{\varepsilon}_{0h_{11/2}}$ is equal to 2.5 MeV. This large gap produces the $Z = 64$ subshell effect, which manifests as a very large excitation energy of the 2_1^+ state. Interestingly, this gap gradually decreases as nuclei move away from ^{146}Gd, revealing a trend in the evolution of the proton shell structure. Similarly, we find a 1.6 MeV gap between the $1g_{7/2}$ and $1d_{5/2}$ orbits in ^{140}Ce, which is responsible for the large excitation energy of the 2_1^+ state.

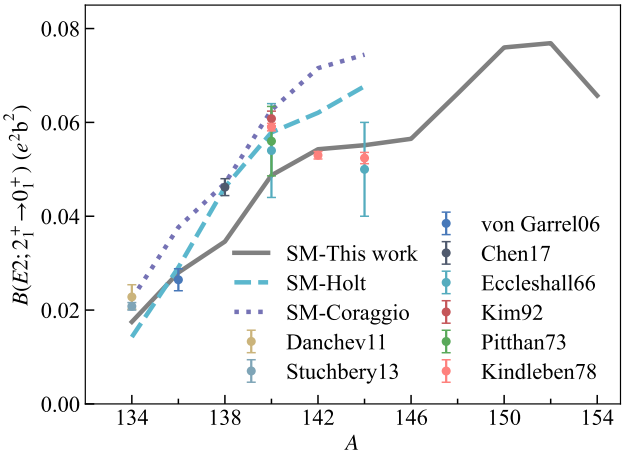

Fig. 4 The electric quadrupole reduced transition probabilities $B(E2; 2_1^+ \to 0_1^+)$ for the $N = 82$ even-even isotones with $Z > 50$. 'SM-Holt" and "SM-Coraggio" represent the SM results in Refs. [12] and [13], respectively. The experimental data are taken from Refs. [26-34].

Fig. 4 compares for the $B(E2; 2_1^+ \to 0_1^+)$ values from the data, the SM results in this work and in Refs. [12-13]. The data are taken from Refs. [26-34]. We see for the lighter $N = 82$ nuclei with $A \leqslant 144$, our SM result is in good agreement with the data within the experimental uncertainties, except that for ^{138}Ba the $B(E2)$ value obtained by our calculation is 25% smaller than the data. On the other hand, the SM results in Refs. [12-13] for ^{134}Te, ^{136}Xe, ^{138}Ba, and ^{140}Ce are in good agreement with the data, but those for ^{142}Nd and ^{144}Sm are too large. The $B(E2; 2_1^+ \to 0_1^+)$ value for the isotones heavier than ^{144}Sm has not been measured. Our SM calculation predicts that the $B(E2; 2_1^+ \to 0_1^+)$ value for ^{146}Gd is close to those for ^{142}Nd and ^{144}Sm, and the value increases rapidly from ^{148}Dy to ^{152}Yb and drops at ^{154}Hf. The $Z = 64$ subshell closure does not lead to a shallow minimum of $B(E2; 2_1^+ \to 0_1^+)$ at ^{146}Gd. This feature is different from the feature in Sn isotopes that there is a shallow minimum near $N = 64$.

4 Summary

In this paper we calculate low-lying level energies and $B(E2; 2_1^+ \rightarrow 0_1^+)$ values for $N = 82$ even-even isotones in the shell model with an effective interaction. The experimental data exhibit two distinct peaks of $E_x(2_1^+)$ at ^{146}Gd and ^{140}Ce. Our shell model results for $E_x(2_1^+)$ and binding energies are in good agreement with the experimental data, while previous shell model results are not as good as ours. Our calculation also well reproduces the $B(E2; 2_1^+ \rightarrow 0_1^+)$ for ^{134}Te, ^{136}Xe, ^{140}Ce, ^{142}Nd, and ^{144}Sm. The calculation and the effective interaction used in this work describe correctly the proton shell structure for the $N = 82$ isotones.

Our HF calculation shows a 2.5 MeV energy gap between the $1d_{5/2}$ and $0h_{11/2}$ orbits in ^{146}Gd. This large gap results in the formation of the $Z = 64$ subshell closure. Similarly, we find a 1.6 MeV energy gap between the $0g_{7/2}$ and $1d_{5/2}$ orbits in ^{140}Ce. Our shell model calculation predicts the $B(E2; 2_1^+ \rightarrow 0_1^+)$ value for ^{146}Gd is close to those for ^{142}Nd and ^{144}Sm, and the values increase rapidly from ^{148}Dy to ^{152}Yb. The existence of the $Z = 64$ subshell does not lead to a shallow minimum of $B(E2; 2_1^+ \rightarrow 0_1^+)$ at ^{146}Gd.

References

[1] OGAWA M, BRODA R, ZELL K, et al. Lowest 2^+ state in $^{146}_{64}Gd_{82}$ and the energy gap at $z = 64$[J]. Phys. Rev. Lett., 1978, 41: 289-292.

[2] CASTEN R F, WARNER D D, BRENNER D S, et al. Relation between the $z = 64$ shell closure and the onset of deformation at $n = 88 - 90$[J]. Phys. Rev. Lett., 1981, 47: 1433-1436.

[3] Evidence for reduced collectivity around the neutron mid-shell in the stable even-mass sn isotopes from new lifetime measurements[J]. Physics Letters B, 2011, 695(1): 110-114.

[4] MORALES I O, VAN ISACKER P, TALMI I. Generalized seniority and e2 transitions in the tin isotopes[J]. Physics Letters B, 2011, 703 (5): 606-608.

[5] BANU A, GERL J, FAHLANDER C, et al. ^{108}Sn studied with intermediate-energy coulomb excitation[J]. Phys. Rev. C, 2005, 72: 061305.

[6] ANSARI A. Study of the lowest 2+ excitations and b (e2) transition strengths in relativistic qrpa for sn-, and pb-isotopes[J]. Physics Letters B, 2005, 623(1-2): 37-42.

[7] ANSARI A, RING P. Lowest lying 2+ and 3- vibrational states in pb, sn, and ni isotopes in relativistic quasiparticle random-phase approximation[J]. Physical Review C, 2006, 74(5): 054313.

[8] TERASAKI J. Qrpa study of low-lying 2+ states of even-even nuclei in neutron-rich sn and ni region[J]. Nuclear Physics A, 2004, 746: 583-586.

[9] IUDICE N L, STOYANOV C, TARPANOV D. E 2 transitions in sn isotopes within the quasiparticle-phonon model[J]. Physical Review C, 2011, 84(4): 044314.

[10] JIANG H, LEI Y, FU G, et al. B (e 2; 0 1+→ 2 1+) values of even-even sn isotopes[J]. Physical Review C, 2012, 86(5): 054304.

[11] TOGASHI T, TSUNODA Y, OTSUKA T, et al. Novel shape evolution in sn isotopes from magic numbers 50 to 82[J]. Physical Review Letters, 2018, 121(6): 062501.

[12] HOLT A, ENGELAND T, OSNES E, et al. Extended shell model calculation for even n= 82 isotones with a realistic effective interaction [J]. Nuclear Physics A, 1997, 618(1-2): 107-125.

[13] CORAGGIO L, COVELLO A, GARGANO A, et al. Shell-model study of the n= 82 isotonic chain with a realistic effective hamiltonian [J]. Physical Review C, 2009, 80(4): 044320.

[14] CHEN Q Y, et al. [Z]. To be published.

[15] JOHNSON C W, ORMAND W E, KRASTEV P G. Factorization in large-scale many-body calculations[J]. Computer Physics Communications, 2013, 184(12): 2761-2774.

[16] JOHNSON C W, ORMAND W E, MCELVAIN K S, et al. Bigstick: A flexible configuration-interaction shell-model code[A]. 2018.

[17] BROWN B, RAE W. The shell-model code nushellx@ msu[J]. Nuclear Data Sheets, 2014, 120: 115-118.

[18] JIA L. Generalized seniority on a deformed single-particle basis[J]. Physical Review C, 2017, 96(3): 034313.

[19] JIA L. Application of the variational principle to a coherent-pair condensate: The bcs case[J]. Physical Review C, 2019, 99(1): 014302.

[20] YU Y, LU Y, FU G, et al. Nucleon-pair truncation of the shell model for medium-heavy nuclei[J]. Physical Review C, 2022, 106 (4): 044309.

[21] TALMI I. Generalized seniority and structure of semi-magic nuclei [J]. Nuclear Physics A, 1971, 172(1): 1-24.

[22] CAPRIO M, LUO F, CAI K, et al. Generalized seniority for the shell model with realistic interactions[J]. Physical Review C, 2012, 85(3): 034324.

[23] JIA L. Practical calculation scheme for generalized seniority[J]. Journal of Physics G: Nuclear and Particle Physics, 2015, 42(11): 115105.

[24] HUANG W, WANG M, KONDEV F G, et al. The ame 2020 atomic mass evaluation (i). evaluation of input data, and adjustment procedures[J]. Chinese Physics C, 2021, 45(3): 030002.

[25] From ensdf database available at http://www.nndc.bnl.gov/ensarchivals/[EB/OL].

[26] RADFORD D, BAKTASH C, BEENE J, et al. Coulomb excitation of radioactive 1 3 2, 1 3 4, 1 3 6 te beams and the low b (e 2) of 136 te [J]. Physical review letters, 2002, 88(22): 222501.

[27] DANCHEV M, RAINOVSKI G, PIETRALLA N, et al. One-phonon isovector 2 1, ms+ state in the neutron-rich nucleus 132 te[J]. Physical Review C, 2011, 84(6): 061306.

[28] STUCHBERY A E, ALLMOND J M, GALINDO-URIBARRI A, et al. Electromagnetic properties of the 2 1+ state in 134 te: Influence of core excitation on single-particle orbits beyond 132 sn[J]. Physical Review C, 2013, 88(5): 051304.

[29] VON GARREL H, VON BRENTANO P, FRANSEN C, et al. Low-lying e 1, m 1, and e 2 strength distributions in xe 124, 126, 128, 129, 130, 131, 132, 134, 136: Systematic photon scattering experiments in the mass region of a nuclear shape or phase transition[J]. Physical Review C, 2006, 73(5): 054315.

[30] CHEN J. Nucl. data sheets, 146, 1 (2017)[EB/OL].

[31] BARENGHI C F. Vortices and the couette flow of helium ii[J]. Physical Review B, 1992, 45(5): 2290.

[32] PITTHAN R. Unelastische streuung von 50 und 65 mev-elektronen an ce, la und pr[J]. Zeitschrift für Physik A Hadrons and nuclei, 1973, 260(4): 283-304.

[33] KINDLEBEN G, ELZE T W. B (e 2)-values of even-a nuclei with 82 neutrons[J]. Zeitschrift für Physik A Atoms and Nuclei, 1978, 286: 415-417.

[34] ECCLESHALL D, YATES M, SIMPSON J. Coulomb excitation of low-energy states in ce, nd and sm isotopes[J]. Nuclear Physics, 1966, 78(3): 481-491.

$N = 82$ 偶偶同中子素 2_1^+ 态的系统性

陈青云[1]，俞一信[1]，郭绍棠[1]，傅冠健[1]，任中洲[1]

(1. 同济大学物理科学与工程学院, 上海 200092;)

摘要：在本文中我们研究质子数在 52 和 72 之间的 $N = 82$ 偶偶同中子素 2_1^+ 态的系统性。我们用原子核壳模型结合单极和多极修正的真实相互作用计算了 0_1^+ 和 2_1^+ 态能级以及电四极约化跃迁几率 $B(E2; 2_1^+ \to 0_1^+)$。我们的计算结果与实验数据非常吻合。我们的研究表明在 ^{146}Gd 中 $Z = 64$ 子壳的能隙为 2.5 MeV。我们预测 ^{146}Gd 的 $B(E2; 2_1^+ \to 0_1^+)$ 值与 ^{142}Nd 和 ^{144}Sm 的值接近，从 ^{148}Dy 到 ^{152}Yb 的 $B(E2)$ 值迅速增大。

关键词：壳模型;$N = 82$ 同中子素;2_1^+ 态能量; 电四极约化跃迁几率

收稿日期：2023-06-19；　修改日期：2023-06-19

基金项目：国家重点研发计划 (2018YFA0404403)；国家自然科学基金资助项目 (12075169,12035011, 11605122)

通信作者：傅冠健，E-mail: gjfu@tongji.edu.cn